

# Development of functional devices using hot spot in $\text{GdBa}_2\text{Cu}_3\text{O}_{7-\delta}$ -based composite ceramics

Tomoichiro Okamoto, Masasuke Takata\*

*Department of Electrical Engineering, Nagaoka University of Technology, 1603-1 Kamitomioka, Nagaoka, Niigata 940-2188, Japan*

Received 10 December 2003; accepted 17 December 2003

Available online 26 June 2004

## Abstract

A hot spot, which is a local area glowing orange, appears in  $\text{LnBa}_2\text{Cu}_3\text{O}_{7-\delta}$  (Ln: rare earth element) ceramic rod when a voltage exceeding a certain value is applied to the rod at room temperature. The rod with the hot spot shows various functional characteristics that give rise to applications in devices such as a constant-current generator, an oxygen sensor. The durability of the rod during a sustained presence of the hot spot is improved upon adding  $\text{BaAl}_2\text{O}_4$  into the  $\text{GdBa}_2\text{Cu}_3\text{O}_{7-\delta}$ . In this paper,  $\text{GdBa}_2\text{Cu}_3\text{O}_{7-\delta}$ -based composite ceramic rod with various  $\text{BaAl}_2\text{O}_4$  contents were prepared by solid-state reaction, and current–voltage characteristics and temperature dependences of resistivity were measured. The minimum electric power required for the hot spot to appear increased with increasing  $\text{BaAl}_2\text{O}_4$  content. From the temperature dependence of the resistivity, temperature just before the hot spot appearance could be successfully estimated. The minimum electric power required for the hot spot to appear can be expected from the temperature dependence of the resistivity of the ceramics, which is useful to design the functional devices exploiting the hot spot.

© 2004 Elsevier Ltd and Techna Group S.r.l. All rights reserved.

**Keywords:** Hot spot; Current–voltage characteristic; Temperature dependence of resistivity; PTCR

## 1. Introduction

$\text{LnBa}_2\text{Cu}_3\text{O}_{7-\delta}$  (Ln: rare earth element), which is well known as the high- $T_c$  superconductor, is a typical non-stoichiometric oxide. Oxygen deficiency,  $\delta$ , increases with increasing temperature above 400 °C [1]. The carrier density decreases with increasing  $\delta$ , which results in a steep increase of the resistivity [2–4]. In other words, the material shows a positive temperature coefficient of resistivity (PTCR).

The present authors observed the phenomenon that a local area of a  $\text{GdBa}_2\text{Cu}_3\text{O}_{7-\delta}$  ceramic rod glows orange once a voltage exceeding a certain value is applied to the rod at room temperature (Fig. 1) [5]. The visible glowing area was named a hot spot. The appearance of the hot spot is related to the PTCR characteristic [5–7].

With increasing voltage the current through the rod decreases abruptly when the hot spot appears, and then remains constant [6–9]. This is possible because the size of a hot

spot with higher resistivity increases linearly with increasing voltage [5–7]. The rod with the hot spot can be used as a constant-current generator without any active component.

The current after the appearance of the hot spot depends on the oxygen partial pressure in ambient atmosphere, which acts as an oxygen sensor without the need for any heating system [6,10].

To enable the practical use of devices utilizing the hot spot, the durability of the rod is very important. The temperature of the hot spot is about 900 °C, which is almost the same as the sintering temperature of  $\text{GdBa}_2\text{Cu}_3\text{O}_{7-\delta}$  [6,8]. Therefore, the  $\text{GdBa}_2\text{Cu}_3\text{O}_{7-\delta}$  rod tends to be molten and broken by a sustained presence of the hot spot. In the preceding paper on this issue, we demonstrated that a ceramic rod composed of  $\text{GdBa}_2\text{Cu}_3\text{O}_{7-\delta}$  and  $\text{BaAl}_2\text{O}_4$  withstood breakage [11]. The improvement of the durability was considered to be related to the high stability of  $\text{BaAl}_2\text{O}_4$  in the hot spot. Barium aluminate is stable up to high temperature (melting point, 1815 °C), and known as a raw material for refractory cement [12], a ferroelectric material [13] and a fluorescent material [14].

To design the devices exploiting the hot spot, the minimum electric power for the functions to be demonstrated is

\* Corresponding author. Tel.: +81-258-47-9509;  
fax: +81-258-47-3604.

E-mail address: takata@vos.nagaokaut.ac.jp (M. Takata).

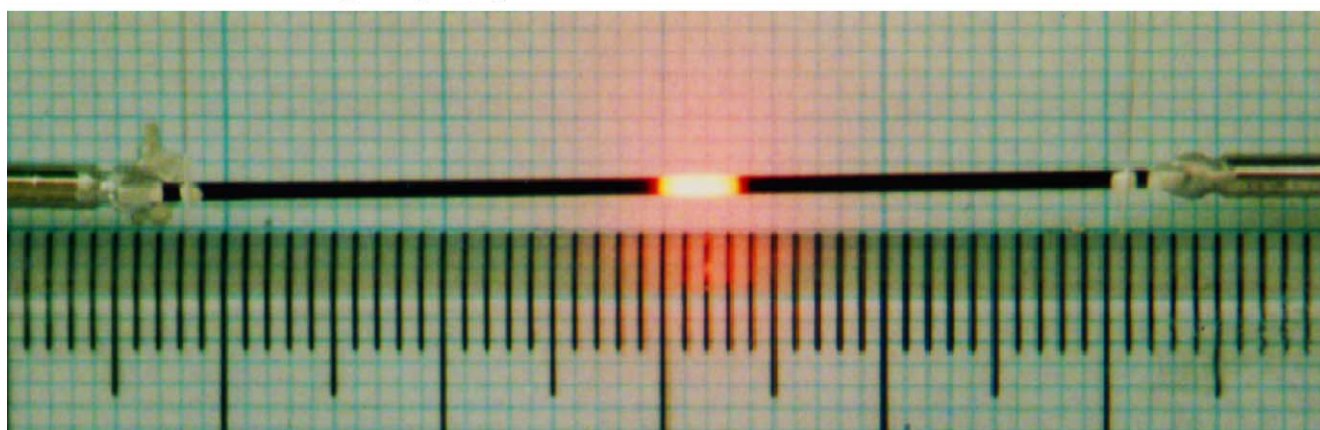
dc 10 V  $\text{GdBa}_2\text{Cu}_3\text{O}_{7-\delta}$ 

Fig. 1. Photograph of a hot spot appearing on a  $\text{GdBa}_2\text{Cu}_3\text{O}_{7-\delta}$  ceramic rod. A dc voltage of 10 V was applied to the rod at room temperature in air.

important. The minimum electric power is directly linked with the appearance mechanism of the hot spot. In the present study,  $\text{GdBa}_2\text{Cu}_3\text{O}_{7-\delta}$ -based composite ceramics with various contents of  $\text{BaAl}_2\text{O}_4$  were prepared by solid-state reaction, and the effect of the  $\text{BaAl}_2\text{O}_4$  on the appearance of hot spot was investigated.

## 2. Experimental procedure

The powders of  $\text{GdBa}_2\text{Cu}_3\text{O}_{7-\delta}$  and  $\text{BaAl}_2\text{O}_4$  were prepared by conventional solid-state reaction. The starting powders  $\text{Gd}_2\text{O}_3$ ,  $\text{BaCO}_3$  and  $\text{CuO}$  (Soekawa Chemical, >99.9% purity) were weighed in the ratio of  $\text{Gd}:\text{Ba}:\text{Cu} = 1:2:3$ , mixed for 2 h in ethanol, dried and then sintered at  $910^\circ\text{C}$  for 10 h in air. The sintered body was then ground into powder to obtain the  $\text{GdBa}_2\text{Cu}_3\text{O}_{7-\delta}$  powder. For the preparation of  $\text{BaAl}_2\text{O}_4$  powder, the powders of  $\text{BaCO}_3$  and  $\text{Al}_2\text{O}_3$  (Soekawa Chemical, >99.9% purity) mixed in the ratio of  $\text{Ba}:\text{Al} = 1:2$  were sintered at  $1000^\circ\text{C}$  in air for 10 h and ground into powder.

The  $\text{GdBa}_2\text{Cu}_3\text{O}_{7-\delta}$  powder was mixed with 0–100 mol%  $\text{BaAl}_2\text{O}_4$  powder, and sintered at  $900^\circ\text{C}$  for 5 h in air. The sintering temperature was set at low to obtain a porous sample in which the hot spot appears easily. The resultant samples were characterized by X-ray diffraction (XRD; Rigaku, RAD-2C), scanning electron microscopy (SEM; JEOL, JSM-5510) and energy dispersive X-ray spectroscopy (EDS; JEOL, JED-2201).

The samples were cut into a rod shape with a cross-section of  $0.65\text{ mm} \times 0.65\text{ mm}$ . The electrical characteristics were measured by a four-probe method with the distance between voltage electrodes being 30 mm.

## 3. Results and discussion

Fig. 2 shows typical XRD pattern of the sample with 70 mol%  $\text{BaAl}_2\text{O}_4$ . All the peaks could be assigned only

to  $\text{GdBa}_2\text{Cu}_3\text{O}_{7-\delta}$  and  $\text{BaAl}_2\text{O}_4$  as well as other samples. From these results, all the resultant samples were considered to be composite ceramics consisting of  $\text{GdBa}_2\text{Cu}_3\text{O}_{7-\delta}$  and  $\text{BaAl}_2\text{O}_4$ .

Fig. 3 shows SEM images and electron probe microanalyzer (EPMA) maps of Cu and Al for the fractured surface of the composite ceramics with 30 and 70 mol% of  $\text{BaAl}_2\text{O}_4$ . In the elemental maps, the white area indicates a high concentration of the elements. The Cu and Al maps were considered to show the distributions of  $\text{GdB}_2\text{C}_3\text{O}_{7-\delta}$  and  $\text{BaAl}_2\text{O}_4$ , respectively. The grains of  $\text{BaAl}_2\text{O}_4$  were distinguished from those of  $\text{GdBa}_2\text{Cu}_3\text{O}_{7-\delta}$ . It was found that the samples had porous microstructures composed of grains of both  $\text{GdBa}_2\text{Cu}_3\text{O}_{7-\delta}$  and  $\text{BaAl}_2\text{O}_4$ .

Fig. 4 shows the current–voltage characteristics of the  $\text{GdBa}_2\text{Cu}_3\text{O}_{7-\delta}$ -based composite ceramic rods with various  $\text{BaAl}_2\text{O}_4$  contents. The arrows indicate breaking of the rods caused by melting. For the rods with  $\text{BaAl}_2\text{O}_4$  content higher than 70 mol%, the electrical resistance was too high to measure the characteristics. The current through the  $\text{GdBa}_2\text{Cu}_3\text{O}_{7-\delta}$  rod increased linearly with increasing

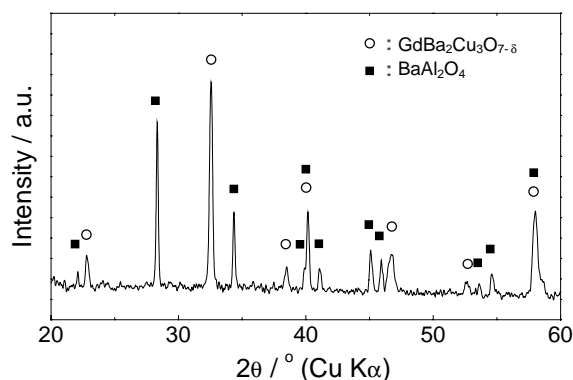


Fig. 2. XRD pattern for the composite ceramics of  $\text{GdBa}_2\text{Cu}_3\text{O}_{7-\delta}$  with 70 mol%  $\text{BaAl}_2\text{O}_4$ . The samples were sintered at  $900^\circ\text{C}$  for 5 h in air. The peaks were attributed only to  $\text{GdBa}_2\text{Cu}_3\text{O}_{7-\delta}$  and  $\text{BaAl}_2\text{O}_4$ .

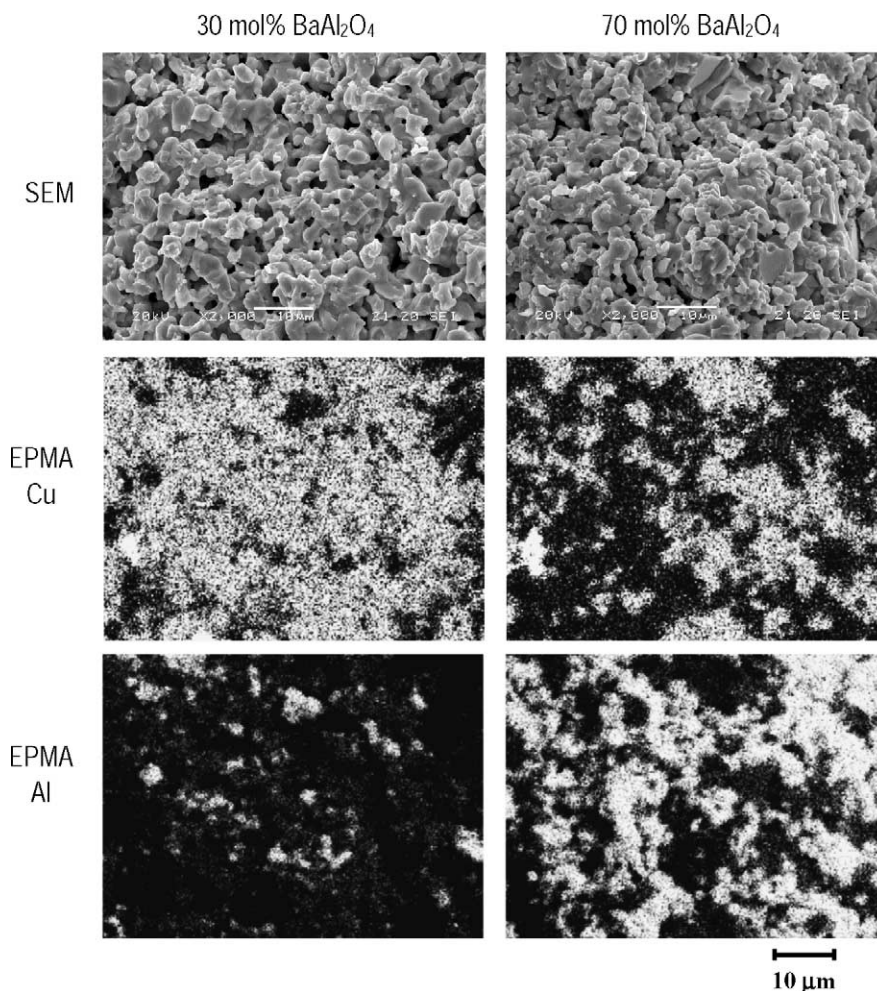


Fig. 3. SEM images and EPMA maps for the fractured surface of  $\text{GdBa}_2\text{Cu}_3\text{O}_{7-\delta}$  composite ceramics with 30 and 70 mol% of  $\text{BaAl}_2\text{O}_4$ . The grains of  $\text{BaAl}_2\text{O}_4$  were distinguished from those of  $\text{GdBa}_2\text{Cu}_3\text{O}_{7-\delta}$ .

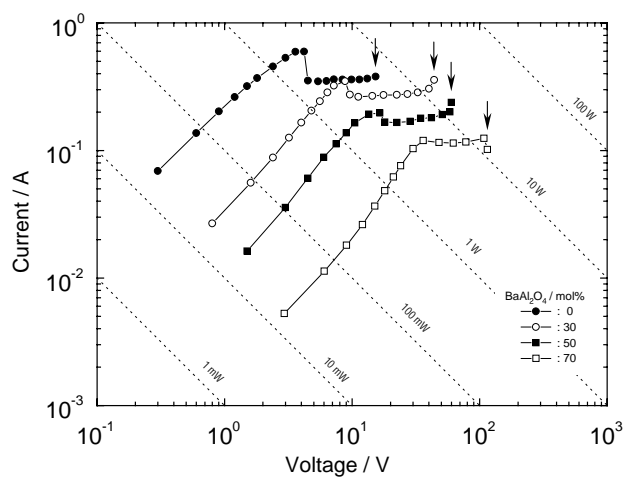


Fig. 4. Current–voltage characteristics for  $\text{GdBa}_2\text{Cu}_3\text{O}_{7-\delta}$  composite ceramic rods with various  $\text{BaAl}_2\text{O}_4$  contents. The arrows indicate breaking of the rods caused by melting. With increasing voltage, the each current increased lineally and decreased abruptly when the hot spot appeared in the rod. After the hot spot appearance, constant-current characteristics were observed.

voltage and decreased abruptly at a certain voltage, and then a hot spot appeared in the rod. With further increasing voltage, the current remained constant. The constant-current characteristic was observed in each rod after the appearance of the hot spot. It is clear that the electrical resistance increased with increasing  $\text{BaAl}_2\text{O}_4$  content. This result suggests that the current pass consisting of the conductive  $\text{GdBa}_2\text{Cu}_3\text{O}_{7-\delta}$  grains is blocked with the insulating  $\text{BaAl}_2\text{O}_4$  grains to a certain extent. The increase of the maximum power indicated by the arrows suggests the improvement of the durability of the rod, which has been described elsewhere [11].

Fig. 5 shows the minimum power required for the hot spot to appear. With increasing the content of  $\text{BaAl}_2\text{O}_4$ , the power increased gradually, and then increased steeply when the content increased over 50 mol%. From this result, it was found that the mixture of  $\text{BaAl}_2\text{O}_4$  affected not only the durability but also the appearance of the hot spot.

The appearance of the hot spot is strongly related to the temperature dependence of the resistivity for the  $\text{GdBa}_2\text{Cu}_3\text{O}_{7-\delta}$ -based composite ceramics, which is shown



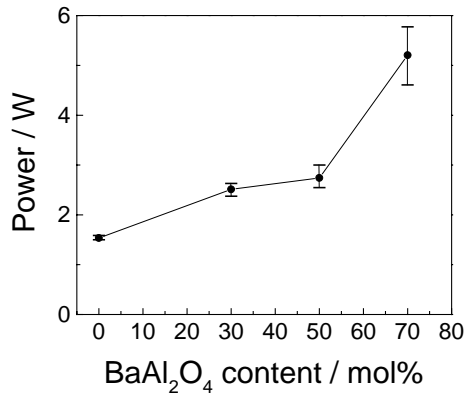


Fig. 5. Relationship between BaAl<sub>2</sub>O<sub>4</sub> content and electric power required for the hot spot to appear. With increasing content, the power increased gradually, and then increased steeply when the content increased over 50 mol%.

in Fig. 6. Each sample showed PTCR when the temperature increased over 400 °C. The appearance of the hot spot is related to such a steep increase in resistivity above a certain temperature [5–7].

The appearance of the hot spot can be described from the viewpoint of heat balance between the generated heat in the rod and the heat dissipated to the environment. The temperatures of the hot and cold regions can be obtained by considering the heat balance of the rod.

$$C \frac{\partial T}{\partial t} = j^2 \rho(T) - W(T) + \frac{\partial}{\partial x} \lambda(T) \frac{\partial T}{\partial x} \quad (1)$$

where  $C$  is the heat capacity per unit volume,  $j$  the current density,  $\rho(T)$  the resistivity,  $\lambda(T)$  the thermal conductivity,

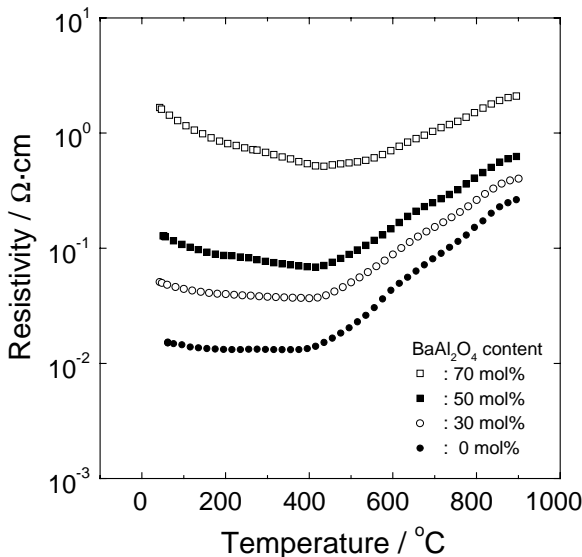


Fig. 6. Temperature dependence of the resistivity for the GdBa<sub>2</sub>Cu<sub>3</sub>O<sub>7-δ</sub> composite ceramics with various contents of BaAl<sub>2</sub>O<sub>4</sub>. The resistivity of all rods increased with increasing temperature over 400 °C. The temperature coefficient of the resistivity over 400 °C decreased with increasing the content.

and  $W(T)$  the heat dissipated to the environment per unit volume [15].

Here, the rod is assumed to be sufficiently long to neglect the heat sinking into electrodes. When the system is in equilibrium ( $\partial T / \partial t = 0$ ), and if each region is assumed to be at a constant uniform temperature ( $(\partial / \partial x) \lambda(T) (\partial T / \partial x) = 0$ ), the balance can be written as

$$j^2 \rho(T) = W(T) \quad (2)$$

The dissipated heat as a function of temperature is written as

$$W(T) = k \{ h(T - T_0) + \sigma(T^4 - T_0^4) \} \quad (3)$$

where  $k = P/A$ ,  $P$  is the perimeter and  $A$  the area of the cross-section of rod,  $h$  the heat transfer coefficient between the rod and the atmosphere,  $T_0$  the ambient temperature, and  $\sigma$  is the Stefan–Boltzmann constant. If the temperature is low, thermal radiation can be neglected and the dissipated heat is approximated by the following equation.

$$W(T) = kh \Delta T \quad (4)$$

where  $\Delta T = T - T_0$ .

Fig. 7 schematically explain the appearance mechanism of the hot spot [6]. To consider the process of the appearance in detail, the relation between the generated and the dissipated heat at each applied voltage as shown in the inset of Fig. 5 is discussed.

①→②: At low voltage,  $j^2 \rho(T)$  curve intersects with  $W(T)$  at one point, and the temperature of the whole rod is slightly higher than  $T_0$ . With increasing applied voltage,  $j$  increases and  $j^2 \rho(T)$  curve shifts upward. When the voltage reaches a certain value, the curve of  $j^2 \rho(T)$  becomes tangent to  $W(T)$  at a metastable temperature  $T_m$ .

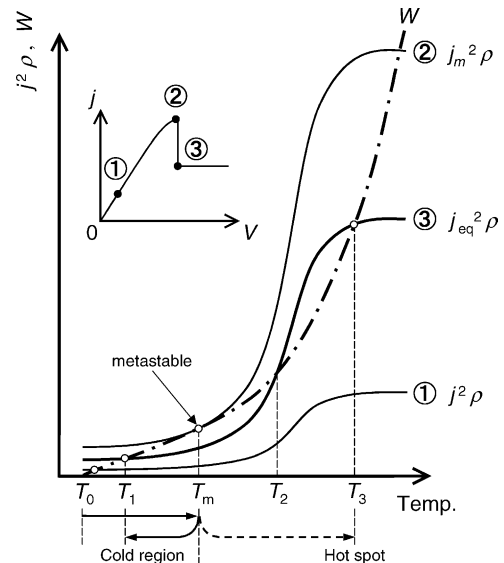


Fig. 7. Schematics of generated joule heat  $j^2 \rho$  with various current densities and dissipated heat  $W$  as a function of temperature [6]. The inset shows typical current density–voltage characteristics. Each  $j^2 \rho$  curve numbered from ① to ③ corresponds to the generated heat at the applied voltage shown in the inset.

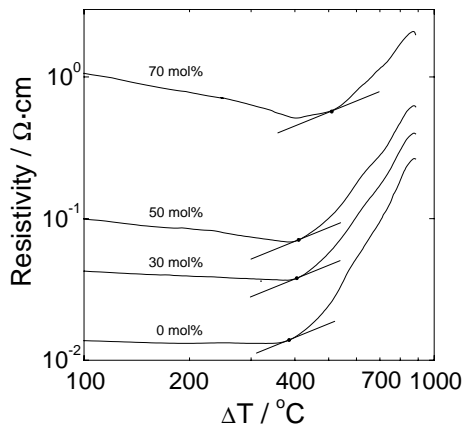


Fig. 8. Schematic estimation of  $T_m$  for the  $\text{GdBa}_2\text{Cu}_3\text{O}_{7-\delta}$  composite ceramics with various contents of  $\text{BaAl}_2\text{O}_4$ . The horizontal axis  $\Delta T$  stands for the difference between the ambient temperature ( $25^\circ\text{C}$ ) and that of the sample.

②→③: When a certain voltage is applied to the rod, it is possible that an certain local area of the rod with the highest resistivity in the rod has a temperature slightly higher than  $T_m$ . The highest resistivity can be caused by the inhomogeneity of local composition, cross-section, microstructure, etc. If there is a slight increase in temperature on the certain area of the rod, the generated heat  $j^2\rho(T)$  is larger than the dissipated heat  $W(T)$ , and the temperature of this area increases further. Then, the resistivity of this area increases because of the PTCR, which leads to a decrease in  $j$ , and  $j^2\rho(T)$  curve shifts downward. As the system reaches equilibrium, the temperature of this area becomes  $T_3$  because of the increase in  $\rho$  which causes the concentration of voltage over this area, while the rest of the rod cools down to  $T_1$  because of the decrease in  $j$ . Therefore,  $T_3$  is the temperature of the hot spot and  $T_1$  is that of the rest.

From above discussion, it is found that the appearance of the hot spot requires the metastable temperature  $T_m$ . Substituting Eq. (4) into Eq. (2), one obtains the heat balance as

$$\log(\rho(T)) = \log(\Delta T) + \log(hk) - 2\log(j) \quad (6)$$

This equation suggests that the  $T_m$  can be estimated from the relation between logarithmic resistivity and logarithmic temperature difference.

Fig. 8 shows schematic estimation of  $T_m$  for the  $\text{GdBa}_2\text{Cu}_3\text{O}_{7-\delta}$  composite ceramics with various contents of  $\text{BaAl}_2\text{O}_4$ . The curves stand for the relationship between logarithmic resistivity and logarithmic temperature difference. The tangent lines have a constant of proportion of 1. Therefore,  $T_m$  can be estimated from the temperature of point of contact between the curve and the tangent line.

Fig. 9 presents the relationship between the minimum electric power required for the hot spot appearance and the

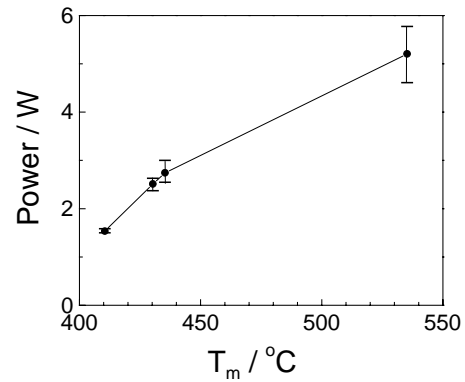


Fig. 9. Relationship between the minimum electric power required for the hot spot to appear and the estimated temperature  $T_m$  from Fig. 8. The values of  $T_m$  were obtained by adding the ambient temperature ( $25^\circ\text{C}$ ) to the temperature obtained in Fig. 8.

estimated temperature  $T_m$  from Fig. 8. The power increased with increasing  $T_m$ . From the results, it was found that the minimum electric power could be expected from the  $T_m$  estimated from the temperature dependence of the resistivity of the ceramics.

#### 4. Conclusion

The  $\text{GdBa}_2\text{Cu}_3\text{O}_{7-\delta}$ -based composite ceramic rods with various  $\text{BaAl}_2\text{O}_4$  contents were prepared by solid-state reaction, and current–voltage characteristics and temperature dependences of resistivity were measured. The temperature of the rod just before the hot spot appearance could be successfully estimated by schematic way. It was found that the electric power require for the hot spot to appear could be expected from the temperature dependence of the resistivity of the ceramics. The expectation of the minimum power for the hot spot appearance is useful to design the functional devices exploiting the hot spot.

#### References

- [1] K. Kishio, J. Shimoyama, T. Hasegawa, K. Kitazawa, K. Fueki, *Jpn. J. Appl. Phys.* 26 (1987) L1228–L1230.
- [2] V.A.M. Brabers, W.J.M. de Jonge, L.A. Bosch, C.v.d. Steen, A.M.W. de Groote, A.A. Verheyen, C.W.H.M. Vennix, *Mater. Res. Bull.* 23 (1988) 197–207.
- [3] A.T. Fiory, M. Gurvitch, R.J. Cava, G.P. Espinosa, *Phys. Rev. B* 36 (1987) 7262–7265.
- [4] T.K. Chaki, M. Rubinstein, *Phys. Rev. B* 36 (1987) 7259–7261.
- [5] T. Okamoto, B. Huybrechts, M. Takata, *Jpn. J. Appl. Phys.* 33 (1994) L1212–L1214.
- [6] M. Takata, Y. Noguchi, Y. Kurihara, T. Okamoto, B. Huybrechts, *Bull. Mater. Sci.* 22 (1999) 593–600.
- [7] H. Sunatori, T. Okamoto, M. Takata, *J. Ceram. Soc. Jpn.* 111 (2003) 217–218.
- [8] Y. Kurihara, Y. Noguchi, M. Takata, *Key Eng. Mater.* 157–158 (1999) 127–134.

- [9] Y. Kurihara, T. Okamoto, B. Huybrechts, M. Takata, *J. Mater. Res.* 11 (1996) 549–551.
- [10] A. Fukuoka, M. Takata, *New Ceram.* 10 (1997) 21–25.
- [11] T. Okamoto, M. Takata, *Key Eng. Mater* 228–229 (2002) 307–310.
- [12] M.M. Ali, S.K. Agarwal, S.K. Handoo, *Cem. Concr. Res.* 27 (1997) 979–982.
- [13] S.Y. Huang, R. Von Der Muhll, J. Ravez, P. Hagenmuller, *J. Phys. Chem. Solids* 55 (1994) 119–124.
- [14] T. Katsumata, R. Sakai, S. Komuro, T. Morikawa, H. Kimura, *J. Cryst. Growth* 198/199 (1999) 869–871.
- [15] G.I. Abramov, A. Gurevich VI, S.I. Zakharchenko, R.G. Mints, L.M. Fisher, *Sov. Phys. Solid State* 27 (1986) 1350–1354.